


Real-Time TECS Gain Tuning Using Steepest Descent Method for Post-Transition Stability in Tiltrotor eVTOLs

Choonghyun Lee ^{1,†,‡} , Ngoc-Phi Nguyen ^{1,‡}, Sangjun Bae ^{2,‡} and Sungkyung Hong ^{3,*}

¹ Department of Convergence Engineering for Intelligent Drone, Sejong University; chung6577@sju.ac.kr

¹ Institute of Mechanical and Electrical Engineering, University of Southern Denmark; npnguyen@sdu.dk

² Department of Drone and Robotics, Sejong Cyber University; sjnbae@gmail.com

* Department of Convergence Engineering for Intelligent Drone, Sejong University; skhong@sejong.ac.kr;

Abstract: Tiltrotor electric Vertical Take-Off and Landing (eVTOL) aircraft encounter significant control challenges during the transition from hover to forward flight, particularly when using open-source autopilot systems like PX4. During this phase, the autopilot employs open-loop tilt angle control and linear weighting of rotor and fixed-wing control outputs, neglecting the aircraft's nonlinear dynamics and resulting in altitude loss. After the transition, when Total Energy Control System (TECS) activates in fixed-wing mode, its fixed gains fail to rapidly correct accumulated errors, exacerbating altitude subsidence. This paper proposes a novel approach to enhance TECS performance after forward transition by dynamically adjusting its gains in real-time using a simple neural network. By adapting gains based on the aircraft's state, this method minimizes altitude loss and stabilizes airspeed and pitch attitude more effectively. Simulation results demonstrate that the neural network-based adaptive TECS significantly reduces altitude subsidence and improves flight stability compared to static gain configurations. This research provides a practical solution to enhance the control performance of tiltrotor eVTOLs, addressing limitations in open-source autopilots and supporting their application in urban air mobility.

Keywords: Tiltrotor eVTOL; TECS; neural networks; adaptive gain tuning; (List three to ten pertinent keywords specific to the article; yet reasonably common within the subject discipline.)

1. Introduction

The development of electric Vertical Take-Off and Landing (eVTOL) aircraft, particularly those with tiltrotor configurations, has gained significant attention due to their potential in urban air mobility and logistics. These hybrid aircraft integrate the vertical lift capabilities of helicopters with the forward flight efficiency of fixed-wing airplanes, necessitating advanced control systems to manage the transition from hover to cruise modes [1].

Open-source autopilot systems, such as PX4, are widely adopted for their accessibility and flexibility. TECS, introduced by Lambregts in 1983 [2], manages total energy—combining kinetic and potential energy—to regulate airspeed and altitude via coordinated throttle and elevator inputs. While effective for fixed-wing aircraft, its application to tiltrotor eVTOLs requires adaptation to address the unique dynamics of the transition phase. Previous studies have validated adaptive TECS strategies for fixed-wing aircraft [3] and proposed modifications for unmanned aerial vehicles [4], yet these approaches have not been explored during the transition phase of tiltrotor eVTOLs.

Received:

Revised:

Accepted:

Published:

Citation: Lastname, F.; Lastname, F.; Lastname, F. Title. *Journal Not Specified* 2025, 1, 0. <https://doi.org/>

Copyright: © 2025 by the authors.

Submitted to *Journal Not Specified* for possible open access publication under the terms and conditions of the Creative Commons Attribution (CC BY) license (<https://creativecommons.org/licenses/by/4.0/>).

In PX4, the transition phase relies on open-loop tilt angle control and linear weighting of multicopter and fixed-wing control outputs, which neglects nonlinear dynamics and leads to altitude loss. TECS activates only after the transition, in fixed-wing mode, where its fixed gains fail to promptly correct errors accumulated during the transition. This study proposes a real-time adaptive TECS gain tuning framework using a simple neural network to address these limitations after forward transition. The neural network dynamically adjusts TECS gains based on the aircraft's current state (e.g., altitude error, airspeed, pitch rate), aiming to minimize altitude loss and ensure rapid stabilization of airspeed and pitch attitude. This approach provides a practical alternative to designing a complex transition control system.

The paper is structured as follows: Section 2 analyzes the transition phase of open-source autopilots and the limitations of TECS implementation. Section 3 details the neural network-based gain tuning methodology. Section 4 presents simulation results comparing the adaptive TECS with conventional methods. Section 5 concludes with implications and future research directions. Through this work, we aim to enhance the reliability and efficiency of control systems for next-generation eVTOL platforms. This study addresses the critical gap in tiltrotor eVTOL control by introducing a neural network-based adaptive TECS framework, offering a novel solution to the challenges of post-transition instability neglected by existing open-source autopilot systems.

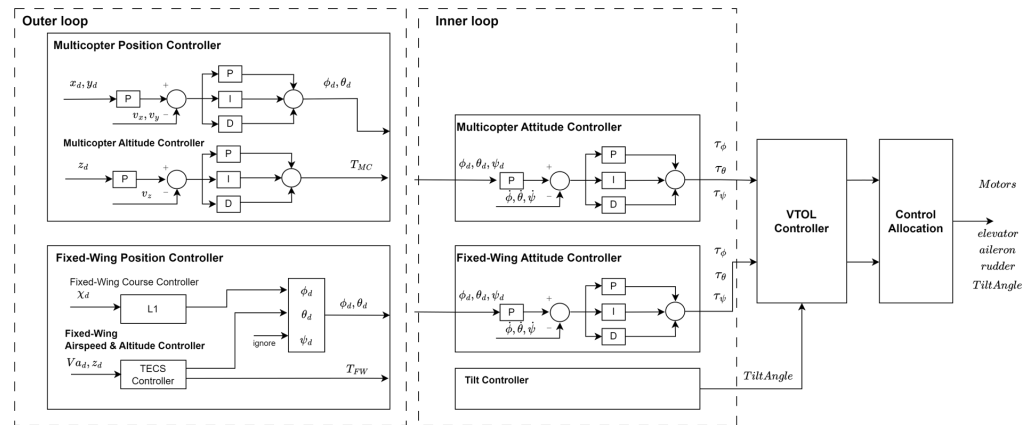


Figure 1. PX4 VTOL Control Structure

2. Literature Review

2.1. Limitations of Current Transition Logic in Open-Source Autopilots

Despite recent advances in open-source autopilot systems such as PX4, the transition control logic for hybrid aircraft, particularly tiltrotor eVTOLs, remains rudimentary. The control architecture relies heavily on open-loop strategies and static gain scheduling, which fail to capture the nonlinear and time-varying dynamics encountered during and after transition phases. This inadequacy forms the basis for the adaptive gain tuning approach proposed in this study.

2.1.1. Analysis of PX4 Transition Phase

The transition phase in open-source autopilots involves two key mechanisms:

- Open Loop Tilt Angle Control

The front rotor of the tilt rotor tilts to a certain angle to achieve airspeed during the transition. Once the transition starting speed (BLENDED_ASPD) is reached, the transition algorithm begins. Until transition completion airspeed, tilt angle keep particular tilt an-

gle(VT_TILT_TRANS). When the transition completion speed (TRANSITION_ASPD) is reached, the switch to fixed-wing mode starts.

- Linear Weighting of Control Outputs

At this point, the outputs for attitude control of the fixed-wing and rotary-wing are divided based on the current airspeed with weighting applied. Once the transition completion speed (TRANSITION_ASPD) is reached, the output of the fixed-wing control takes over completely.

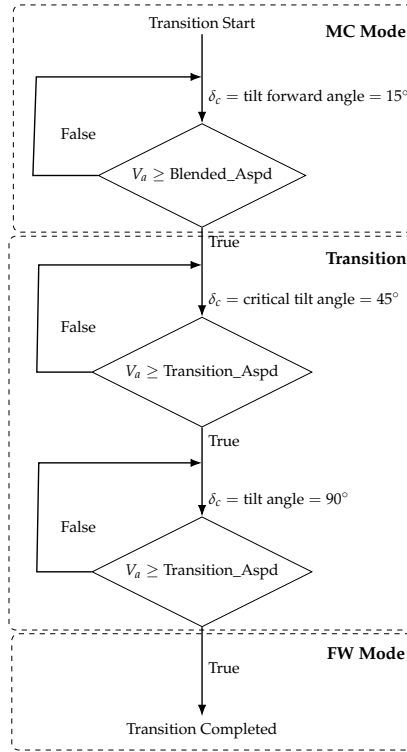


Figure 2. Flowchart for the Transition Process in Flight Modes

In the transition phase, the open-source method does not consider the aircraft's nonlinear dynamics, such as rotor tilt angle changes, which can lead to altitude loss and instability post-transition.

2.2. Total Energy Control System (TECS)

The Total Energy Control System (TECS) is a control strategy used in aircraft to manage their total energy, which consists of potential energy ($E_p = mgh$) and kinetic energy ($E_k = \frac{1}{2}mv^2$). TECS regulates airspeed and altitude by coordinating throttle and pitch inputs: throttle adjusts the total energy, while pitch controls the distribution of energy between altitude and speed.

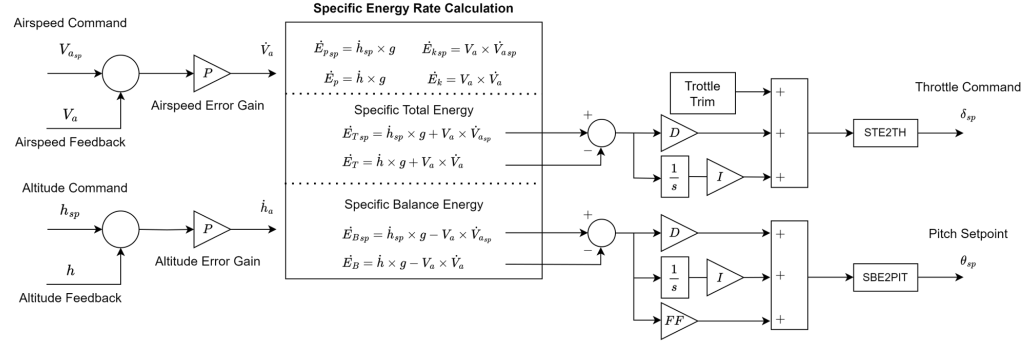


Figure 3. PX4 TECS Control Structure

In the Open-Source autopilot framework, TECS remains inactive during the transition phase of tiltrotor eVTOLs and only activates once the aircraft fully enters fixed-wing mode.

2.2.1. TECS Control Structure

TECS manages two primary functions:

- **Total Energy Control:** Adjusts throttle to regulate the total specific energy rate ($\dot{E}_T = \dot{E}_P + \dot{E}_K$), where:
 - $\dot{E}_P = \dot{h}g$ (potential energy rate, linked to altitude change),
 - $\dot{E}_K = v\dot{v}$ (kinetic energy rate, linked to speed change).
- **Balance Energy Control:** Adjusts pitch to control the balance specific energy rate ($\dot{E}_B = \dot{E}_T - \dot{E}_K$), ensuring proper energy distribution between altitude and airspeed.

The setpoints for these energy rates are defined as:

$$\dot{E}_{Tsp} = \dot{h}_{sp}g + v_a\dot{v}_{asp}, \quad \dot{E}_{Bsp} = \dot{h}_{sp}g - v_a\dot{v}_{asp} \quad (1)$$

where \dot{h}_{sp} is the desired altitude rate, v_a is the current airspeed, and \dot{v}_{asp} is the desired airspeed rate.

The control outputs—thrust (δ_{sp}) and pitch (θ_{sp})—are calculated as:

$$\delta_{sp} = \left(D_T(\dot{E}_{Tsp} - \dot{E}_T) + I_T \int (\dot{E}_{Tsp} - \dot{E}_T) dt + T_{cruise} \right) \frac{1}{\dot{E}_{T,max} - \dot{E}_{T,min}} \quad (2)$$

$$\theta_{sp} = \left(D_B(\dot{E}_{Bsp} - \dot{E}_B) + I_B \int (\dot{E}_{Bsp} - \dot{E}_B) dt + ff_B \dot{E}_{Bsp} \right) \frac{1}{v_a g} \quad (3)$$

where:

- D_T, I_T : Derivative and integral gains for specific total energy rate,
- D_B, I_B : Derivative and integral gains for specific balance energy rate,
- ff_B : Feedforward gain,
- T_{cruise} : Cruise thrust,
- $\dot{E}_{T,max} = g \times \text{max_climb_rate}$, $\dot{E}_{T,min} = g \times \text{max_descent_rate}$: Limits on energy rates.

For tiltrotors, the transition phase introduces unique dynamics, such as rotor tilt angle changes, which affect the balance between \dot{E}_P and \dot{E}_K . Fixed gains, as used in PX4's default TECS, fail to adapt to these rapid changes, resulting in delayed altitude recovery and instability post-transition.

3. Methodology

3.1. Adaptive Gain Tuning via Steepest Descent

To mitigate the limitations of static TECS gains in addressing the nonlinear dynamics of tiltrotor eVTOLs during the post-transition phase, this study proposes a real-time gain tuning methodology employing the steepest descent method. The proposed approach dynamically adjusts the proportional (K_p) and integral (K_i) gains of TECS based on critical flight states—such as altitude error, airspeed deviation, and pitch rate—thereby minimizing altitude loss and substantially enhancing stability immediately following the transition to fixed-wing mode, while providing a resource-efficient solution for open-source autopilot systems.

The steepest descent method minimizes the error function defined as $E = \frac{1}{2}(r(t) - y_s(t))^2$, where $r(t)$ represents the reference state and $y_s(t)$ denotes the system output. The update rules for the gains are formulated as:

$$\frac{dK_p}{dt} = -\eta_p \frac{\partial E}{\partial K_p}, \quad \frac{dK_i}{dt} = -\eta_i \frac{\partial E}{\partial K_i}$$

This formulation draws inspiration from early work by Ahn and Thanh (2005), who applied the steepest descent method to tune PID gains for a pneumatic artificial muscle (PAM) manipulator, using a single-layer structure initially described as a neural network [11]. More recent advancements, such as those by Alagoz et al. (2018), further refined this approach for nonlinear TRMS control, employing a fourth-degree polynomial to approximate system dynamics [8]. The stability of the proposed approach is substantiated by Yağmur and Alagoz (2017), who established the Lyapunov stability of continuous-time gradient descent dynamics for $\forall \eta > 0$ [9]. Specifically, by defining the Lyapunov function $V = E$, the time derivative is:

$$\frac{dV}{dt} = \frac{\partial E}{\partial K_p} \frac{dK_p}{dt} + \frac{\partial E}{\partial K_i} \frac{dK_i}{dt} = -\eta_p \left(\frac{\partial E}{\partial K_p} \right)^2 - \eta_i \left(\frac{\partial E}{\partial K_i} \right)^2 \leq 0$$

This guarantees the stability of the proposed method for positive learning rates.

3.1.1. Motivation for the Steepest Descent Method

During the transition from multicopter to fixed-wing mode, the aircraft undergoes significant aerodynamic shifts and thrust vector changes, resulting in residual effects that persist into the post-transition phase. Fixed-gain TECS, activated only after the transition to fixed-wing mode, is insufficient to address these dynamic variations, often leading to sub-optimal altitude control and delayed stabilization. The steepest descent method facilitates real-time adaptation by iteratively optimizing the gains based on current error metrics (e.g., altitude and energy rate deviations), providing a robust and resource-efficient solution for open-source platforms such as PX4. By directly minimizing the error function, this method ensures rapid adaptation to the dynamic flight conditions immediately following the transition, thereby substantially enhancing post-transition stability.

3.1.2. Steepest Descent Gain Update Formulation

The steepest descent method optimizes the gains by minimizing the cost function:

$$J(k) = \frac{1}{2}(\dot{E}_{sp}(k) - \dot{E}(k))^2 \quad (4)$$

where $\dot{E}_{sp}(k)$ represents the desired energy rate and $\dot{E}(k)$ denotes the actual energy rate. The control structure, inspired by Ahn and Thanh (2005), consists of a control optimizer

that adjusts the gains and an adaptation optimizer that estimates the system dynamics, as depicted in Figure 4.

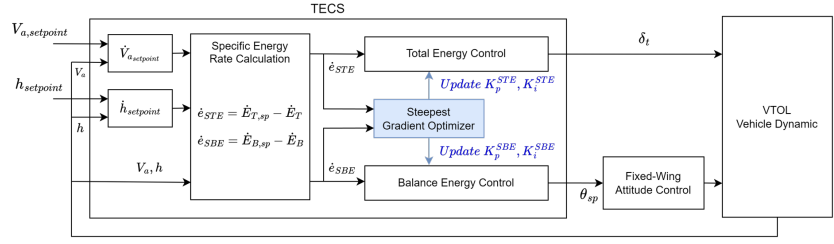


Figure 4. Block diagram of gradient descent optimizer control, adapted from Ahn and Thanh (2005) [11].

where $x(k) = K_p(k)e_p(k) + K_i(k)e_i(k)$, $e_p(k) = \dot{E}_{sp}(k) - \dot{E}(k)$, $e_i(k) = \sum \int e_p(k) dt$, and Y_g is a tuning parameter shaping the sigmoid curve, as illustrated in Figure 5. The update rules for the gains are:

$$f(x) = \frac{2(1 - e^{-xY_g})}{Y_g(1 + e^{-xY_g})} \quad (5)$$

with

$$x(k) = K_p(k)e_p(k) + K_i(k)e_i(k), \quad e_p(k) = \dot{E}_{sp}(k) - \dot{E}(k), \quad e_i(k) = \sum \int e_p(k) dt \quad (6)$$

The update rules for the controller gains are given by:

$$K_p(k+1) = K_p(k) - \eta_p \frac{\partial J(k)}{\partial K_p(k)}, \quad K_i(k+1) = K_i(k) - \eta_i \frac{\partial J(k)}{\partial K_i(k)} \quad (7)$$

where the partial derivatives are evaluated as:

$$\frac{\partial J(k)}{\partial K_p(k)} = -e_p(k)f'(x(k))e_p(k), \quad \frac{\partial J(k)}{\partial K_i(k)} = -e_p(k)f'(x(k))e_i(k) \quad (8)$$

and

$$f'(x) = \frac{4e^{-xY_g}}{(1 + e^{-xY_g})^2} \quad (9)$$

The learning rates η_p and η_i govern the convergence speed and must be selected to ensure both stability and responsiveness.

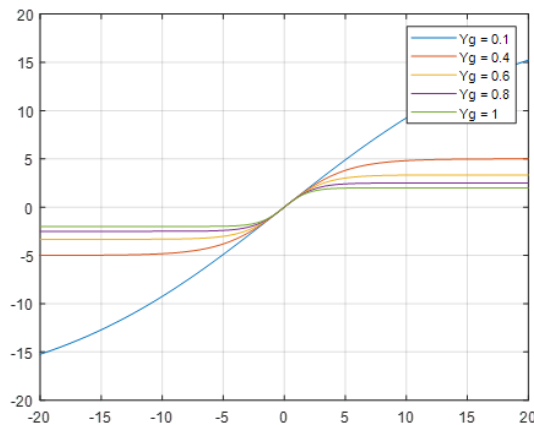


Figure 5. Sigmoid function shapes for different Y_g values.

3.2. Implementation and Validation

The proposed method was implemented and tested using PX4 simulations, focusing on the post-transition phase in fixed-wing mode. Performance was evaluated by comparing altitude stability and recovery time against the default fixed-gain TECS.

4. Simulation Model

4.1. Aircraft Configuration and Longitudinal Dynamics

The simulation framework is designed to model and analyze the longitudinal dynamics of a tiltrotor eVTOL platform, specifically focusing on altitude, airspeed, and pitch attitude. The aircraft model reflects a conventional tiltrotor configuration with transition-capable rotors and fixed-wing surfaces, parameterized based on typical subscale demonstrators. The key physical parameters used in simulation are listed in Table 1.

Physical Properties	
Symbol	Value
m	5.22 kg
J_x	1.229 kg·m ²
J_y	0.1702 kg·m ²
J_z	0.8808 kg·m ²
J_{xz}	0.9343 kg·m ²
S_{wing}	0.75 m ²
b	2.10 m
\bar{c}	0.3571 m

Table 1. Physical Properties

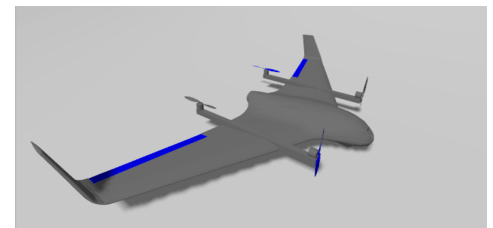


Figure 6. Tiltrotor Gazebo model

Figure 7. Aircraft Model Parameters and Tiltrotor Gazebo Model

where m is the mass, J_x, J_y, J_z, J_{xz} are the moments of inertia, S_{wing} is the wing area, b is the wing span, and \bar{c} is the mean aerodynamic chord. The aerodynamic coefficients are also provided in Table 1.

Aerodynamic Coefficients

Symbol	Value
C_{L_0}	0.0867
C_{L_α}	4.02
C_{L_q}	3.8954
$C_{L_{\delta_e}}$	0.278
C_{D_0}	0.0197
C_{D_α}	0.0791
$C_{D_{\alpha^2}}$	1.06

Symbol	Value
C_{D_q}	0.0
$C_{D_{\delta_e}}$	0.0633
C_{m_0}	0.0302
C_{m_α}	-0.126
C_{m_q}	-1.3047
$C_{m_{\delta_e}}$	-0.206

Table 2. Aerodynamic Coefficients of the Aircraft Model

where C_{L_0} is the lift coefficient at zero angle of attack, C_{L_α} is the lift coefficient per unit angle of attack, C_{L_q} is the lift coefficient per unit pitch rate, $C_{L_{\delta_e}}$ is the lift coefficient per unit elevator deflection, C_{D_0} is the drag coefficient at zero angle of attack, C_{D_α} is the drag coefficient per unit angle of attack, $C_{D_{\alpha^2}}$ is the drag coefficient per unit angle of attack squared, C_{D_q} is the drag coefficient per unit pitch rate, $C_{D_{\delta_e}}$ is the drag coefficient per unit elevator deflection, C_{m_0} is the moment coefficient at zero angle of attack, C_{m_α} is the moment coefficient per unit angle of attack, C_{m_q} is the moment coefficient per unit pitch rate, and $C_{m_{\delta_e}}$ is the moment coefficient per unit elevator deflection.

The aerodynamic coefficients C_L , C_D , and C_m are computed as follows:

$$C_L = C_{L_0} + C_{L_\alpha} \alpha + C_{L_q} \frac{q\bar{c}}{2v} + C_{L_{\delta_e}} \delta_e \quad (10)$$

$$C_D = C_{D_0} + C_{D_\alpha} \alpha + C_{D_{\alpha^2}} \alpha^2 + C_{D_q} \frac{q\bar{c}}{2v} + C_{D_{\delta_e}} \delta_e \quad (11)$$

$$C_m = C_{m_0} + C_{m_\alpha} \alpha + C_{m_q} \frac{q\bar{c}}{2v} + C_{m_{\delta_e}} \delta_e \quad (12)$$

These expressions allow the lift, drag, and pitching moment coefficients to be evaluated dynamically based on instantaneous flight conditions, including angle of attack α , pitch rate q , and elevator deflection δ_e . The aerodynamic forces and moments acting on the aircraft are calculated using the following equations:

$$L = \frac{1}{2} \rho v^2 S C_L, \quad D = \frac{1}{2} \rho v^2 S C_D, \quad M = \frac{1}{2} \rho v^2 S C_m \quad (13)$$

where L is the lift force, D is the drag force, M is the pitching moment, ρ is the air density, v is the airspeed, and S is the wing area.

4.2. Control Architecture

The control architecture of the tiltrotor eVTOL is mode-dependent and composed of cascaded feedback loops tailored to the vehicle's flight configuration. During vertical flight (Multicopter mode), PID-based controllers regulate body angular rates and altitude, while during forward flight (Fixed-Wing mode), the control switches to a fixed-wing attitude controller complemented by a Total Energy Control System (TECS) to manage coupled airspeed and altitude dynamics. This hierarchical structure allows for smooth transition and robustness across flight modes.

- **Multicopter Flight Mode:**
 - *Attitude Stabilization:* A cascaded PID controller regulates roll, pitch, and yaw rates using angular rate feedback.
 - *Altitude Hold:* A proportional-integral (PI) controller tracks desired altitude by modulating vertical thrust.
- **Fixed-Wing Flight Mode:**
 - *Attitude Control:* A pitch attitude controller maintains longitudinal stability using elevator surface deflection.
 - *Energy Management:* TECS regulates total and balance energy rates by coordinating throttle and pitch commands.

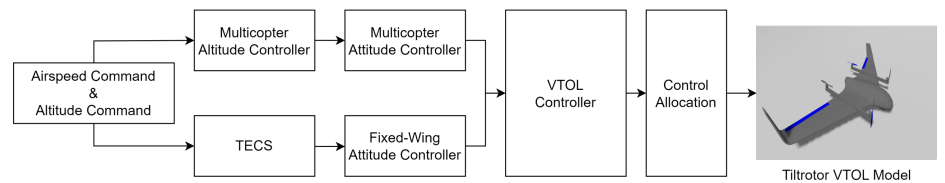


Figure 8. Control System Diagram

This architecture enables mode-specific control tuning and ensures a seamless handover between multicopter and fixed-wing control laws during the transition phase. Figure 8 presents a high-level overview of the control system architecture used in simulation.

5. Simulation Results

5.1. Simulation Setup

The simulation was conducted using MATLAB Simulink. The aircraft model was evaluated under three configurations: (1) the PX4 default fixed-gain TECS, (2) a manually tuned fixed-gain TECS, and (3) the proposed Steepest Descent Adaptive TECS. The simulation targeted the post-transition phase, where the aircraft transitions from multicopter to fixed-wing mode at a predetermined airspeed. The initial conditions were derived from the transition phase, with parameters governing this phase meticulously defined to establish the simulation conditions.

To ensure realistic and optimal performance, specific parameters were configured for both the Vertical Take-Off and Landing (VTOL) transition and the Total Energy Control System (TECS) gain tuning. The VTOL parameters, which govern the transition dynamics from multicopter to fixed-wing mode, include the critical tilt angle, transition thrust, blended airspeed, and transition airspeed. These values were selected based on typical configurations for tiltrotor electric VTOL (eVTOL) aircraft. Similarly, the TECS parameters, including learning rates, sigmoid shaping factors, and initial gains, were selected to optimize the steepest descent method's adaptability and ensure stability during gain tuning. Table 3 provides a detailed summary of these parameters and their values used in the simulation.

Table 3. Simulation Parameters for VTOL Transition and TECS Gain Tuning

Parameter	Value
VTOL Parameters	
Critical Tilt Angle	50 degrees
Transition Thrust	0.35
Blended Airspeed (BLENDED_ASPD)	8 m/s
Transition Airspeed (TRANSITION_ASPD)	15 m/s
TECS Parameters	
η_{ste} (STE Learning Rate)	0.000001
η_{sbe} (SBE Learning Rate)	0.000001
γ_g^{ste} (STE Sigmoid Parameter)	0.3
γ_g^{sbe} (SBE Sigmoid Parameter)	0.2
Initial K_p^{ste} (STE Proportional Gain)	0.8
Initial K_i^{ste} (STE Integral Gain)	0.02
Initial K_p^{sbe} (SBE Proportional Gain)	1.2
Initial K_i^{sbe} (SBE Integral Gain)	0.20
Default K_p^{ste} (Default STE Proportional Gain)	0.8
Default K_i^{ste} (Default STE Integral Gain)	0.02
Default K_p^{sbe} (Default SBE Proportional Gain)	1.2
Default K_i^{sbe} (Default SBE Integral Gain)	0.20

The VTOL parameters, such as Transition Thrust, blended airspeed (BLENDED_ASPD), and transition airspeed (TRANSITION_ASPD) are critical for ensuring a smooth and stable transition phase. These are complemented by the TECS parameters, which enable the neural network to dynamically adjust gains in response to altitude and energy rate errors. The values presented in Table 3 were implemented in the simulation to evaluate the performance of the proposed adaptive TECS gain tuning method.

5.2. TECS State Response

Figure 9 illustrates the altitude and airspeed responses over the simulation period (0-100 sec). The steepest descent-based TECS shows faster altitude recovery compared to the fixed-gain TECS, indicating the effectiveness of the adaptive gain tuning in mitigating

altitude loss during the critical post-transition phase. Both methods stabilize airspeed at a similar rate, underscoring the effectiveness of the steepest descent optimization for altitude control.

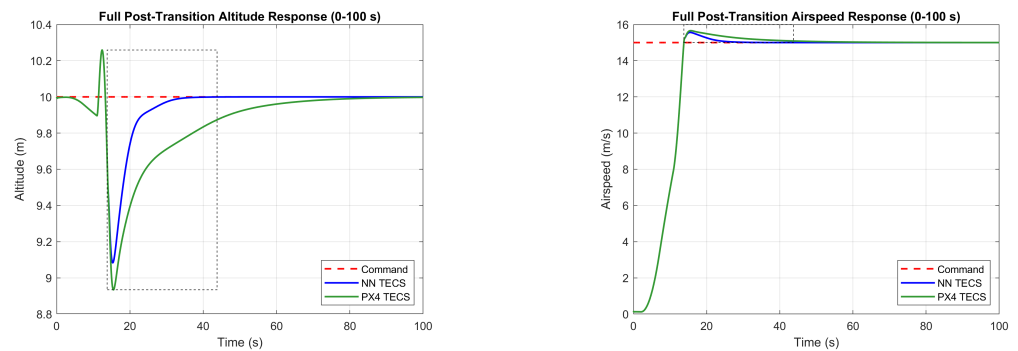


Figure 9. TECS State Response: Altitude and Airspeed Comparison.

5.3. Flight Mode

Figure 10 illustrates the transition from multicopter to fixed-wing mode, where TECS is activated in fixed-wing mode.

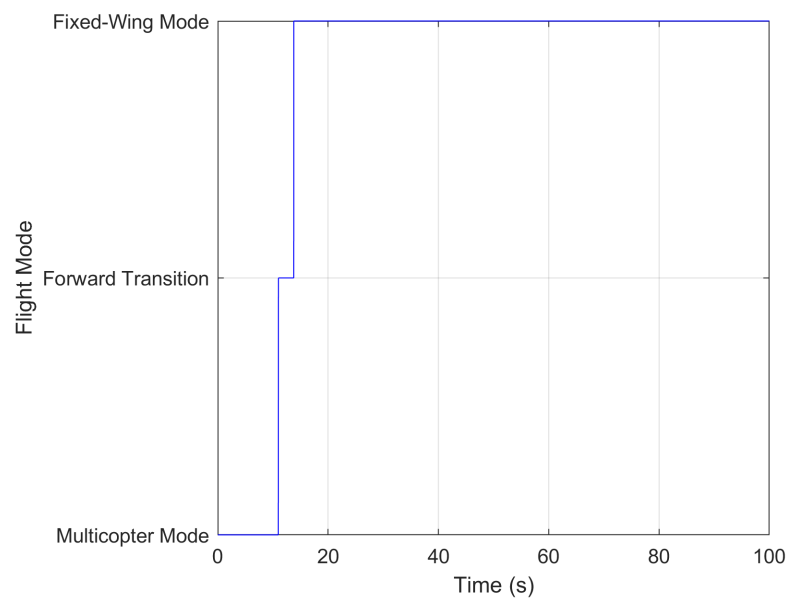


Figure 10. Flight Mode Transition: Multicopter to Fixed-Wing Mode.

As depicted in Figure 10, the aircraft enters fixed-wing mode at 13.8 seconds. The transition phase is critical for the aircraft's stability and performance, and the steepest descent-based adaptive TECS substantially enhances the aircraft's response during this phase.

5.4. Energy Rate Error Response

Figures 11 and 12 show the specific total energy rate (STE) and specific balance energy rate (SBE) error responses, respectively. The steepest descent-based TECS demonstrates faster reduction in both STE and SBE errors, leading to improved altitude and airspeed recovery, showcasing its enhanced stability in the post-transition phase.

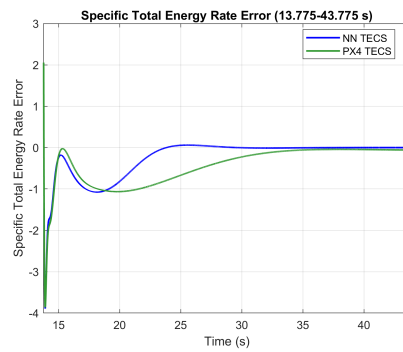


Figure 11. Specific Total Energy Rate Error

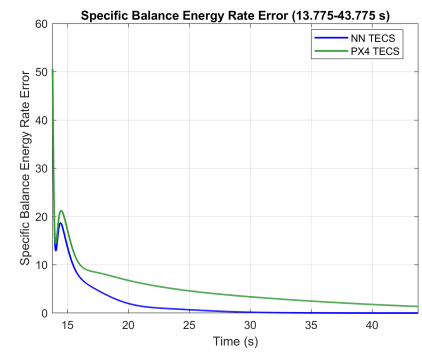


Figure 12. Specific Balance Energy Rate Error

5.5. TECS Control Outputs

Figure 13 and Figure 14 present the thrust and pitch outputs of the TECS control system, respectively. These plots illustrate the control inputs applied post-transition, highlighting the neural network's ability to adjust these outputs for improved stability.

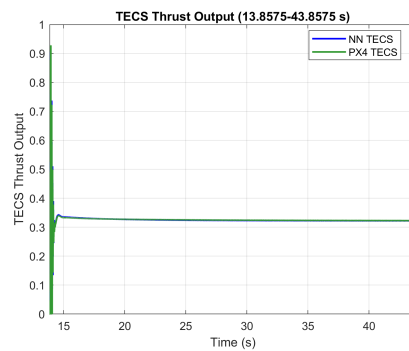


Figure 13. Thrust Output

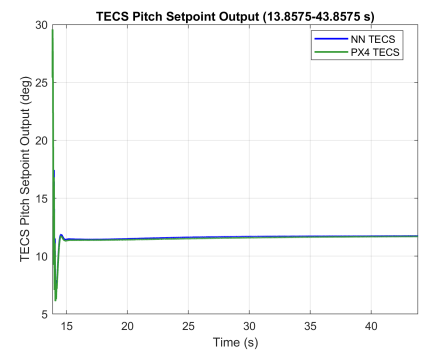


Figure 14. Pitch Setpoint Output

5.6. TECS Gain Tuning

The TECS gain tuning process is illustrated in Figure 15, 16. The neural network dynamically adjusts the proportional and integral gains based on the altitude and energy rate errors, leading to improved performance during the post-transition phase.

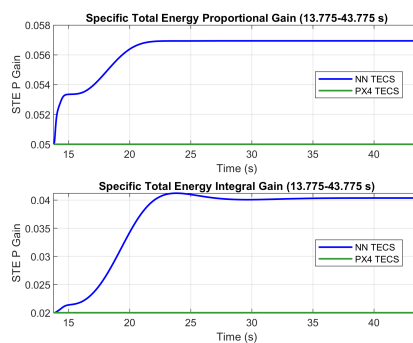


Figure 15. Total Energy Gain

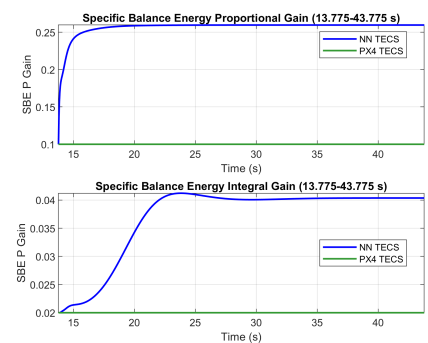


Figure 16. Balance Energy Gain

The gain tuning process is critical for ensuring the TECS can adapt to the changing dynamics of the aircraft during the transition phase. The neural network's ability to learn and adjust these gains in real-time significantly enhances the overall performance of the TECS.

5.7. Sensitive Analysis

The neural network-based adaptive TECS gain tuning method was tested under various conditions to evaluate its robustness and sensitivity to different flight states. The results demonstrate consistent performance across different scenarios, highlighting the method’s adaptability and reliability.

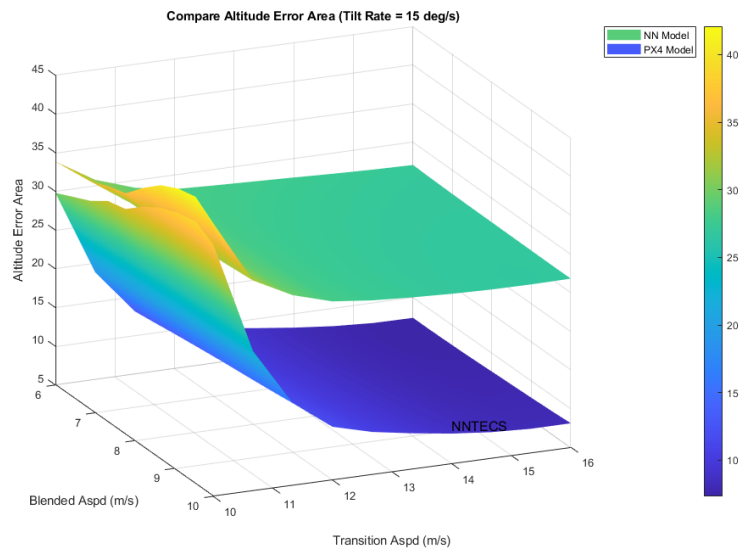


Figure 17. Sensitive Analysis: Neural Network TECS Performance under Different Flight States.

6. Discussion

7. Conclusions

This section is not mandatory, but can be added to the manuscript if the discussion is unusually long or complex.

8. Patents

Author Contributions: For research articles with several authors, a short paragraph specifying their individual contributions must be provided. The following statements should be used “Conceptualization, X.X. and Y.Y.; methodology, X.X.; software, X.X.; validation, X.X., Y.Y. and Z.Z.; formal analysis, X.X.; investigation, X.X.; resources, X.X.; data curation, X.X.; writing—original draft preparation, X.X.; writing—review and editing, X.X.; visualization, X.X.; supervision, X.X.; project administration, X.X.; funding acquisition, Y.Y. All authors have read and agreed to the published version of the manuscript.”, please turn to the [CRediT taxonomy](#) for the term explanation. Authorship must be limited to those who have contributed substantially to the work reported.

Funding: Please add: “This research received no external funding” or “This research was funded by NAME OF FUNDER grant number XXX.” and and “The APC was funded by XXX”. Check carefully that the details given are accurate and use the standard spelling of funding agency names at <https://search.crossref.org/funding>, any errors may affect your future funding.

Institutional Review Board Statement: In this section, you should add the Institutional Review Board Statement and approval number, if relevant to your study. You might choose to exclude this statement if the study did not require ethical approval. Please note that the Editorial Office might ask you for further information. Please add “The study was conducted in accordance with the Declaration of Helsinki, and approved by the Institutional Review Board (or Ethics Committee) of NAME OF INSTITUTE (protocol code XXX and date of approval).” for studies involving humans. OR “The animal study protocol was approved by the Institutional Review Board (or Ethics Committee) of NAME OF INSTITUTE (protocol code XXX and date of approval).” for studies involving animals. OR

“Ethical review and approval were waived for this study due to REASON (please provide a detailed justification).” OR “Not applicable” for studies not involving humans or animals.

Informed Consent Statement: Any research article describing a study involving humans should contain this statement. Please add “Informed consent was obtained from all subjects involved in the study.” OR “Patient consent was waived due to REASON (please provide a detailed justification).” OR “Not applicable” for studies not involving humans. You might also choose to exclude this statement if the study did not involve humans.

Written informed consent for publication must be obtained from participating patients who can be identified (including by the patients themselves). Please state “Written informed consent has been obtained from the patient(s) to publish this paper” if applicable.

Data Availability Statement: We encourage all authors of articles published in MDPI journals to share their research data. In this section, please provide details regarding where data supporting reported results can be found, including links to publicly archived datasets analyzed or generated during the study. Where no new data were created, or where data is unavailable due to privacy or ethical restrictions, a statement is still required. Suggested Data Availability Statements are available in section “MDPI Research Data Policies” at <https://www.mdpi.com/ethics>.

Acknowledgments: This work was supported by Future Space Navigation & Satellite Research Center through the National Research Foundation funded by the Ministry of Science and ICT, the Republic of Korea (2022M1A3C2074404).

This research was supported by Basic Science Research Program through the National Research Foundation of Korea(NRF) funded by the Ministry of Education(2020R1A6A1A03038540)

This work was supported by the IITP(Institute of Information & Coummunications Technology Planning & Evaluation)-ITRC(Information Technology Research Center) grant funded by the Korea government(Ministry of Science and ICT)(IITP-2025-RS-2024-00437494).

Conflicts of Interest: Declare conflicts of interest or state “The authors declare no conflicts of interest.” Authors must identify and declare any personal circumstances or interest that may be perceived as inappropriately influencing the representation or interpretation of reported research results. Any role of the funders in the design of the study; in the collection, analyses or interpretation of data; in the writing of the manuscript; or in the decision to publish the results must be declared in this section. If there is no role, please state “The funders had no role in the design of the study; in the collection, analyses, or interpretation of data; in the writing of the manuscript; or in the decision to publish the results”.

Abbreviations

The following abbreviations are used in this manuscript:

- MDPI Multidisciplinary Digital Publishing Institute
- DOAJ Directory of open access journals
- TLA Three letter acronym
- LD Linear dichroism

Appendix A

Appendix A.1

The appendix is an optional section that can contain details and data supplemental to the main text—for example, explanations of experimental details that would disrupt the flow of the main text but nonetheless remain crucial to understanding and reproducing the research shown; figures of replicates for experiments of which representative data are shown in the main text can be added here if brief, or as Supplementary Data. Mathematical proofs of results not central to the paper can be added as an appendix.

Table A1. This is a table caption.

Title 1	Title 2	Title 3
Entry 1	Data	Data
Entry 2	Data	Data

Appendix B

All appendix sections must be cited in the main text. In the appendices, Figures, Tables, etc. should be labeled, starting with “A”—e.g., Figure A1, Figure A2, etc.

References

1. Author 1, T. The title of the cited article. *Journal Abbreviation* **2008**, *10*, 142–149.

2. Author 2, L. The title of the cited contribution. In *The Book Title*; Editor 1, F., Editor 2, A., Eds.; Publishing House: City, Country, 2007; pp. 32–58.

3. Author 1, A.; Author 2, B. *Book Title*, 3rd ed.; Publisher: Publisher Location, Country, 2008; pp. 154–196.

4. Author 1, A.B.; Author 2, C. Title of Unpublished Work. *Abbreviated Journal Name* year, phrase indicating stage of publication (submitted; accepted; in press).

5. Title of Site. Available online: URL (accessed on Day Month Year).

6. Author 1, A.B.; Author 2, C.D.; Author 3, E.F. Title of presentation. In Proceedings of the Name of the Conference, Location of Conference, Country, Date of Conference (Day Month Year); Abstract Number (optional), Pagination (optional).

7. Author 1, A.B. Title of Thesis. Level of Thesis, Degree-Granting University, Location of University, Date of Completion.

8. B. B. Alagoz, A. Tepajakov, G. Kavuran, and H. Alisoy, “Adaptive Control of Nonlinear TRMS Model by Using Gradient Descent Optimizers,” in *2018 International Conference on Artificial Intelligence and Data Processing (IDAP)*, pp. 1–6, IEEE, 2018.

9. N. Yağmur and B. B. Alagoz, “Comparison of Solutions of Numerical Gradient Descent Method and Continuous Time Gradient Descent Dynamics and Lyapunov Stability,” *Journal Name*, 2017.

10. K. Shimizu, H. Nukumi, and S. Ito, “Direct Steepest Descent Control of Nonlinear Dynamical Systems,” *IFAC Proceedings*, vol. 28, no. 14, pp. 801–806, 1995.

11. K. K. Ahn and T. D. C. Thanh, “Nonlinear PID Control to Improve the Control Performance of the Pneumatic Artificial Muscle Manipulator Using Neural Network,” *Journal of Mechanical Science and Technology*, vol. 19, no. 1, pp. 106–115, 2005.

Disclaimer/Publisher’s Note: The statements, opinions and data contained in all publications are solely those of the individual author(s) and contributor(s) and not of MDPI and/or the editor(s). MDPI and/or the editor(s) disclaim responsibility for any injury to people or property resulting from any ideas, methods, instructions or products referred to in the content.